

Trypsin-Free Cultivation of 3D Mini-Tissues in an Adaptive Membrane Bioreactor

Suzana Djeljadini, Theresa Lohaus, Marcel Gausmann, Sebastian Rauer, Michael Kather, Bernd Krause, Andrij Pich, Martin Möller, and Matthias Wessling*

The production of large scaffold-free tissues is a key challenge in regenerative medicine. Nowadays, temperature-responsive polymers allow intact tissue harvesting without needing proteolytic enzymes. This method is limited to tissue culture plastic with limited upscaling capacity and plain process control. Here, a thermoresponsive hollow fiber membrane bioreactor is presented to produce large scaffold-free tissues. Intact tissues, rich in cell-to-cell connections and ECM, are harvested from a poly(*N*-vinylcaprolactam) microgel functionalized poly(ether sulfone)/poly(vinylpyrrolidone) hollow fiber membrane by a temperature shift. The harvested 3D tissues adhere in successive cultivation and exhibit high vitality for several days. The facile adsorptive coating waives the need for extensive surface treatment. The research is anticipated to be a starting point for upscaling the production of interconnected tissues enabling new opportunities in regenerative medicine, large-scale drug screening on physiological relevant tissues, and potentially opening new chances in cell-based therapies.

1. Introduction

Scaffold-free 3D tissues are of great interest for the regenerative medicine, particularly in cellular therapies such as tissue reconstruction in ocular or corneal, cardiac patches, and bladder augmentation.^[1–3] Scaffold containing tissues, for instance, often face the challenge of unwanted host responses or the interfering in cell–cell interactions, cell assembly, and extracellular matrix (ECM) alignment.^[4] Several other factors such as immunogenicity, degradation rate, toxicity of degradation products, host inflammatory responses, fibrous tissue formation due to scaffold degradation or mechanical mismatch with the surrounding tissue are important to consider when engineering scaffold-based tissues. Scaffold-free tissues offer the potential of recapitulating the complex features of in

vivo tissues and thus are of great importance for in vitro models to explore human tissue physiology and pathophysiology.^[5] When creating tissue models with human-based cells, drug screenings are likely to be more efficient and safe prior to clinical trials in humans.^[5] Moreover, human-based in vitro models can likely replace animal testing and thus reduce the gap between cell cultures and physiological tissues. Therefore offering the potential to bridge the gap between animal models and human studies, thereby supporting and adding in the understanding the underlying mechanisms of different pathological conditions.^[5,6]

Major fabrication techniques for scaffold-free cell tissues are, e.g., spheroids, 3D printing, or the cell sheet engineering approach invented in the 1990s.^[7–9] Spheroids or organoids are created by the aggregation of a high number of cells and were intensively studied by Sutherland et al. as an in vitro carcinoma model.^[10,11] Spheroids were used to screen low performing drugs from the promising drug candidates prior to animal and clinical studies.^[12] Further, spheroids can serve as building blocks in 3D bioprinting to engineer 3D tissue constructs by conventional layer-by-layer technique.^[7] However, challenges in spheroid manufacturing are the control over the spheroid size and the longevity of spheroids as compaction prevents efficient nutrient transport into the core.^[8]


Another approach to engineer scaffold-free tissues is the cell sheet engineering technique, which offers a possibility to engineer cell sheets rich in cell-to-cell connections and ECM. In conventional cell cultivation processes, proteolytic enzymes

S. Djeljadini, T. Lohaus, M. Gausmann, S. Rauer, M. Kather, Prof. M. Wessling
Aachener Verfahrenstechnik
Chair of Chemical Process Engineering
RWTH Aachen University
Forckenbeckstrasse 51, Aachen 52074, Germany
E-mail: manuscripts.cvt@avt.rwth-aachen.de

S. Djeljadini, M. Kather, Prof. A. Pich, Prof. M. Möller, Prof. M. Wessling
DWI-Leibniz Institute for Interactive Materials
Forckenbeckstraße 50, Aachen 52074, Germany

Dr. B. Krause
Baxter International Inc.
Research and Development
Holger-Crafoord-Straße 26, Hechingen 72379, Germany

Prof. A. Pich
Institute of Technical and Macromolecular Chemistry
RWTH Aachen University
Worringerweg 2, Aachen 52074, Germany

 The ORCID identification number(s) for the author(s) of this article can be found under <https://doi.org/10.1002/adbi.202000081>.

© 2020 The Authors. Advanced Biosystems published by Wiley-VCH GmbH. This is an open access article under the terms of the Creative Commons Attribution-NonCommercial-NoDerivs License, which permits use and distribution in any medium, provided the original work is properly cited, the use is non-commercial and no modifications or adaptations are made.

DOI: 10.1002/adbi.202000081

are used to harvest adherent cells, but this is accompanied by isolated, scattered cells and degradation of ECM.

By the cell sheet engineering technology, thermoresponsive polymers such as poly(*N*-isopropylacrylamide) (PNIPAM) are used to detach whole cell sheets with intact ECM by changing the temperature.^[13,14] A change in temperature triggers the amount of the water molecules surrounding hydrophobic isopropyl domains of PNIPAM chains and thereby inverts protein adhesion, which enables detachment of adherent cells without the need for proteolytic enzymes.^[9] At 37 °C above the lower critical solution temperature (LCST) the hydrophobic isopropyl groups of PNIPAM chains are in contact with both water and polymer segments, whereas below the LCST the isopropyl groups are surrounded by water.^[15,16] Lowering the temperature below the LCST 34 °C for PNIPAM, 32 °C for poly(*N*-vinylcaprolactam) (PVCL) the polymer chains become better solvated by water molecules.^[15,17] This effect also tunes the adhesive properties toward ECM proteins, resulting in less protein adhesion below LCST and improved adhesion above LCST. However, this enzymatic-free cell harvesting technology is mostly applied on planar technologies or microcarrier systems,^[14] and the development of 3D tissues currently relies on stacking the formed planar sheets by a cumbersome process.

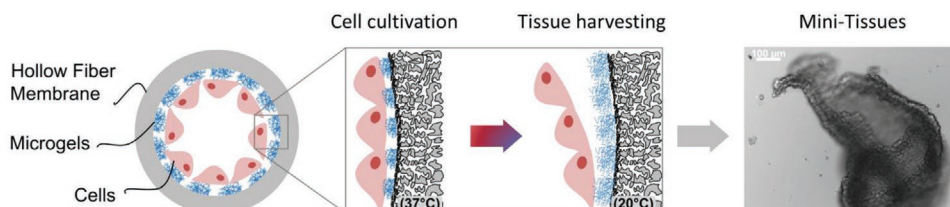
Cellular therapies strongly rely on techniques to expand primary cells obtained from a patient or donor *ex vivo*. Especially mesenchymal stem cells occur only in low numbers in bone marrow, yet they exhibit very promising capabilities for regenerative therapies.^[18] Therapeutic dosages, however, will likely amount to 10⁹–10¹⁰ cells per treatment, thus requiring high cell expansion techniques.^[19] Cell cultivation processes are predominantly performed on planar surfaces, which are restricted in upscaling and always present a danger of dedifferentiation. The limited surface area further lowers the capacity to achieve a large number of tissues, which is required for cellular-based therapies. Besides the low cultivation area, the other major challenge encountered in the currently used methods, which limits upscaling, is mass transfer to and from the tissues. However, efficient mass transport is a crucial aspect of cell cultivation processes. The supply of sufficient nutrients, e.g., oxygen and metabolites such as glucose and amino acids, and the removal of inhibiting by-products is an elementary part in controlling cell cultivation processes and designing reactors.^[20–22] In addition to essential nutrients, sufficient oxygen supply is crucial as it has a poor solubility in the culture medium.^[5] Thus, an unstirred cell culture medium causes a significant diffusion barrier for oxygen, even in 2D-cell monolayer cultivation.^[5] Homogeneous flow distribution and sufficient residence time, allowing radial diffusion of chemical species, are important aspects for reactor systems.^[23]

In the past, several bioreactors were designed for stem cell engineering. Well-known cultivation systems for anchorage-dependent cells are stirred tank reactors, spinner flasks, or rotating wall vessel reactors in combination with microcarriers, microencapsulation-based bioreactors, packed-bed bioreactors, and hollow fiber bioreactors.^[20,22] In comparison to flask-based systems, these bioreactors allow closed bioprocess control, online monitoring and are suitable for long-term cultivation. A major challenge that all systems have in common is the harvesting of adherent cells as proteolytic enzymes are necessary for detachment.

Although hollow fiber bioreactors are complex and scale-up is challenging, they still have unique advantages such as controlled (low) shear environment, mimicking cellular microenvironment through perfusion mode, increased surface-to-volume ratio, and high packing density.^[20]

There were several approaches where porous membranes were used to recapitulate the physiology of organs such as the artificial liver, -kidney, -artery, or -vasculature.^[24–27] A “living membrane” was developed for an artificial kidney device to support dialysis therapies by removing uremic toxins.^[24] For this, a tight monolayer of living renal cells was successfully grown on poly(ether sulfone) (PES) hollow fiber membranes and provided active cationic transport through the membrane, which is essential for the removal of uremic cationic metabolites. In another approach, a membrane-based perfusion bioreactor served as a mediator.^[25] On the one hand, it provided surface areas for different cell types, such as endothelial cells on the lumen side and smooth muscle cells on the outer side. On the other hand, the membrane served as an *in vivo* model to study the crosstalk between different cell types, mimicking physiological conditions. In the work of Bettahalli, membranes were used as artificial capillaries to provide large 3D tissues with sufficient nutrients and complex multilayer cell constructs were engineered with the help of hollow fiber membranes.^[28,29] The review paper of Eghbali et al. highlights the potential of porous membranes for engineering large 3D tissues and provides a profound study on different membrane configurations for different cell types, which is also supported by computational studies.^[30] However, such type of hollow fiber bioreactors have never been used for engineering scaffold-free large tissues.

In this work, we present a new concept of combining the well-defined bioreactor environment of hollow fiber membranes with temperature-responsive microgels to produce large and scaffold-free tissues (**Scheme 1**). Here, biocompatible poly(ether sulfone) / poly(vinylpyrrolidone) (PES/ PVP) hollow fiber membranes are applied and coated with aqueous temperature-responsive PVCL microgels in a facile adsorptive



Scheme 1. Concept of an adaptive hollow fiber membrane bioreactor with temperature-triggered adhesion modulation to produce large scaffold-free tissues. By switching the temperature from 37 to >32 °C, the microgels undergo volume phase transition and increase their swelling degree, what reduces the adhesion toward ECM proteins and allows noninvasive harvesting process for 3D mini-tissues.

coating process. Aqueous microgels are stimuli-responsive colloidal networks that respond to changes in pH, temperature, or light by abrupt change in swelling degree, stiffness, or gel size.^[31,32] Due to their unique properties, the potential applications of microgels are divers such as in oil recovery, catalysis, biomaterials, and bioactive coatings.^[33,34] In this work, temperature-responsive microgels combined with hollow fiber membrane are used to harvest tissues noninvasively without the need of proteolytic enzymes by modulating the temperature. By switching the temperature from 37 °C to >32 °C, the microgels undergo a volume phase transition and increase their swelling degree, what reduces the adhesion toward ECM proteins. The tissue detaches and by applying a controlled flow in the custom-made bioreactor viable scaffold-free tissues can be harvested.

2. Results and Discussion

2.1. Sterilization and Microgel Cytocompatibility

Before microgel-coated membranes can be tested for scaffold-free tissue engineering, two important criteria must be met in advance: the cytocompatibility of the microgels and a working sterilization technique. A typical phase transition behavior for untreated thermoresponsive microgels can be obtained from **Figure 1a**. The synthesized PVCL microgels had a hydrodynamic radius of ≈ 200 nm at 25 °C and ≈ 80 nm at 37 °C, measured with dynamic light scattering (DLS). The volume phase transition temperature (VPTT) of this microgel sample was around 32 °C as estimated by the differentiation of the $R_h = f(T)$ function. The suitability of sterilizing microgels was tested with steam sterilization and UV treatment, presented in **Figure 1b**. The hydrodynamic radius of microgels is very sensitive to the change in the chemical structure or crosslink density. Therefore, we decided to use DLS and compare the hydrodynamic radii of microgels before and after sterilization. The hydrodynamic radii of PVCL microgels measured below and above VPTT were ≈ 200 and ≈ 80 nm, respectively, indicating that both sterilization techniques do not affect strongly the microgels properties (**Figure 1b**). Above the VPTT, the particle distribution of sterilized microgels shows no significant deviation to untreated microgels. This narrow distribution is due to the fact that the microgels are in a collapsed state containing ≈ 10 – 15% water in their interior. In this state, the fuzzy surface of microgels becomes more smooth and microgels behave more like colloidal objects with hard sphere morphology.^[35] In contrast to that, below the VPTT the microgel size distribution is broader as the gels are surrounded by a diffuse shell with dangling chains. For the swollen state, it can be noted that UV treatment slightly decreases particle size distribution while steam sterilization does not. UV treatment may induce additional crosslinking in microgels by the radical recombination and this effect induces the reduction of the hydrodynamic radii. Steam sterilization was already proven to be suitable for PNIPAM microgels, which can also be concluded for PVCL microgels according to the DLS data.^[36] Also, steam sterilization is a common, feasible, and widely used technique in bioprocess engineering and is therefore chosen to be the standard treatment for the present work.

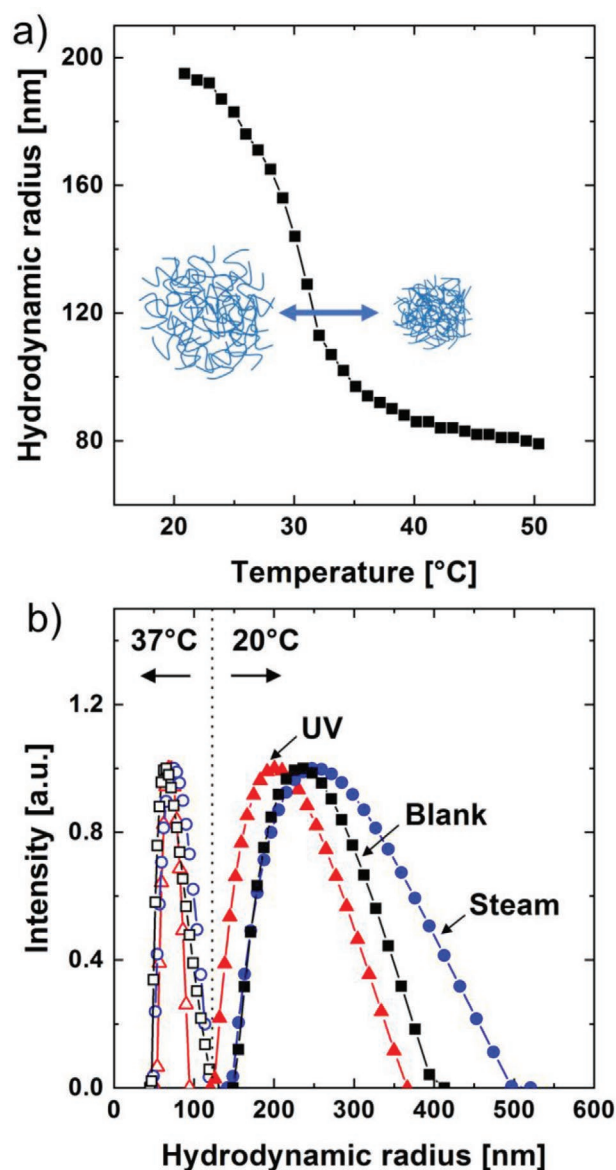


Figure 1. Representative diagram of phase transition behavior of temperature-responsive PVCL microgels. a) Typical temperature-triggered change of hydrodynamic radii for PVCL microgels from the swollen ($T < \text{VPTT}$) to the collapsed ($T > \text{VPTT}$) state. b) Representative particle size distribution of PVCL microgels: untreated (square), steam sterilized (cube) and UV treated (triangle), above (open symbols) and below (closed symbols) the VPTT. Data were obtained from DLS measurements.

Hence, hollow fiber membranes were coated with PVCL microgels, integrated into a custom made bioreactor and steam sterilized at 121 °C. Afterward, a stress test was conducted by filling the whole hollow fiber membrane bioreactor (HFMB) system with cell culture medium without the presence of antibiotics and incubated at 37 °C. Medium samples were taken daily and verified for contamination with a bright field microscope. The system remained sterile for more than 13 d and stopped afterward with a successful sterility test.

The assembly of the HFMB and the used materials can be obtained from **Figure S3** in the Supporting Information.

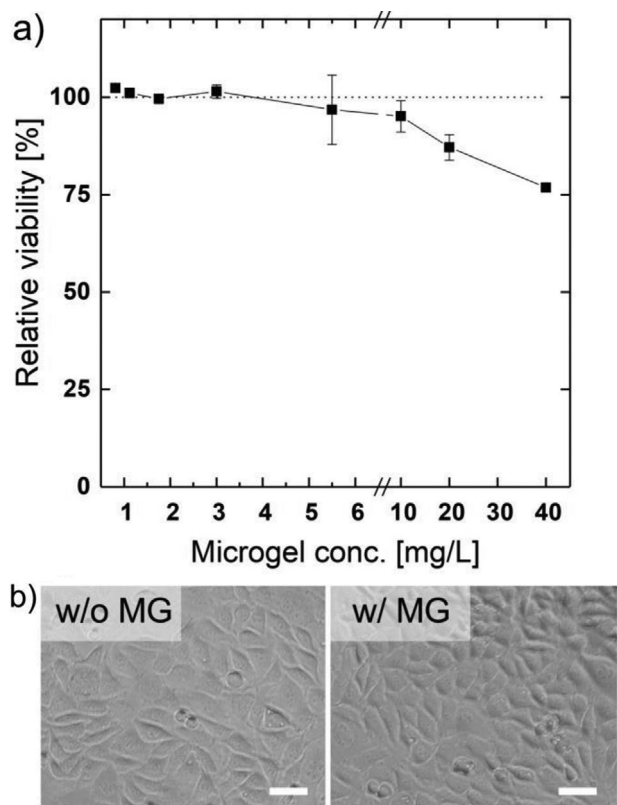


Figure 2. a) Cytocompatibility of PVCL microgels, tested according to DIN10993-5, 2009, with an XTT Cell Proliferation Assay Kit assay. L929 cells were seeded in triplicates (technical replicate) at a concentration of 10^4 cells per well in a 96 well plate and exposed to various concentrations of PVCL microgels for 1 d. Error bars represent standard deviation, $n = 3$. b). Bright-field images of L929 cells without microgels (w/o MG, left picture) and exposed to 40 mg L^{-1} microgels (w/ MG, right picture). Scale bar: $100 \mu\text{m}$.

PNIPAM is a widely used water-swallowable polymer, but the monomers are known to be cytotoxic, as they are prone to produce toxic products when hydrolyzed. In contrast, PVCL is known to be biocompatible and less prone to degradation into cytotoxic compounds, as they do not form any amide compounds under hydrolysis but rather carboxylic acids.^[37,38] This was also confirmed by the conducted cytotoxicity test presented in Figure 2a. We observed no significant reduction in L929 cell viability caused by the PVCL microgels. There was a significant effect of microgel concentration on tissue viability (analysis of variance: $F = 12.2$, d.f. = 8, 21, $p < 0.001$). However, the post hoc Tukey test revealed that there was no significant difference between the control group and the other microgel concentration treatments (Tukey multiple comparison test, $p > 0.05$) (see Table S1, Supporting Information), with the exception of the 20 mg L^{-1} and the 40 mg L^{-1} microgel concentration treatment group. For all test groups, except for the highest microgel concentration (40 mg L^{-1}), the cell vitality was above 80%. Beyond that, cell morphology was investigated by bright-field microscopy, and no significant alterations were discovered for L929 cells, whether they were cultured with microgels (at highest concentration 40 mg L^{-1}) or not (Figure 2b). Thus, all tested concentrations are considered noncytotoxic.

2.2. Formation of a Homogenous Microgel Layer on a Porous Membrane

The membranes used in this work are asymmetric porous PES/PVP membranes, which are kindly provided by Baxter International Inc. The cross-section view of the hollow fiber membrane reveals the sponge-like asymmetric structure, as seen in Figure 3a. In previous work, it was already demonstrated that a stable microgel layer was successfully applied on micro- and ultrafiltration polyethersulfone hollow fiber membranes by dead-end mode filtration.^[39] In the same way, Barth et al. established a procedure of applying monolayers of microgels on PES flat sheet membranes.^[40]

PVCL is very stable against hydrolysis and good biocompatibility was reported.^[37,38] Therefore, PVCL allows a straightforward coating process by adsorption.

In this work, PES hollow fiber membranes were coated according to Menne and Lohaus^[39,41] by dynamic adsorption in dead-end mode inside-out filtration. The presence of microgels is confirmed from the cross-section view of the coated membrane, where an additional layer consisting of PVCL microgels is visible (Figure 3b). The obtained layer thickness of $\approx 80 \pm 5 \text{ nm}$ correlates well with the hydrodynamic radius of the microgels in the collapsed state (Figure 1a), showing that a monolayer of microgels was formed on the membrane surface. The coating procedure also resulted in a homogeneous PVCL layer on the membrane surface, as shown in Figure 3d. While the untreated membrane still shows pores (Figure 3c), the coated membrane is completely covered with PVCL microgels (Figure 3d).

2.3. Temperature-Response of Membranes

In previous works, it was shown that membrane behavior could be tuned by filtering thermoresponsive PVCL microgels onto a porous membrane support, allowing control over the flow and membrane resistance.^[39,41] This temperature-dependent switching of the microgels results in a shift of the hydraulic resistance that can be shown by pure water permeability

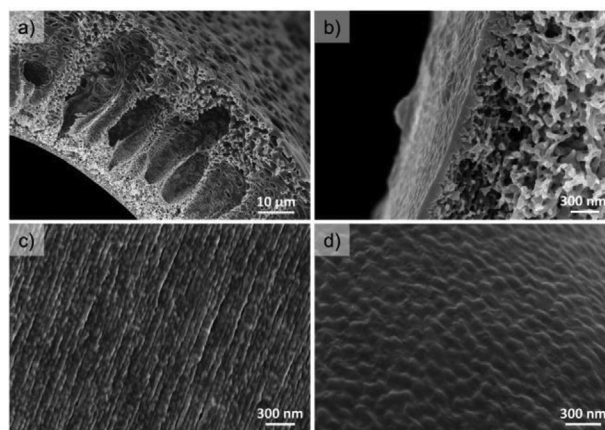


Figure 3. Adsorptive microgel coating on a porous PES/PVP hollow fiber membrane. SEM images of different views: a,b) cross-section and c,d) top view of uncoated (left) and coated (right) hollow fiber membrane.

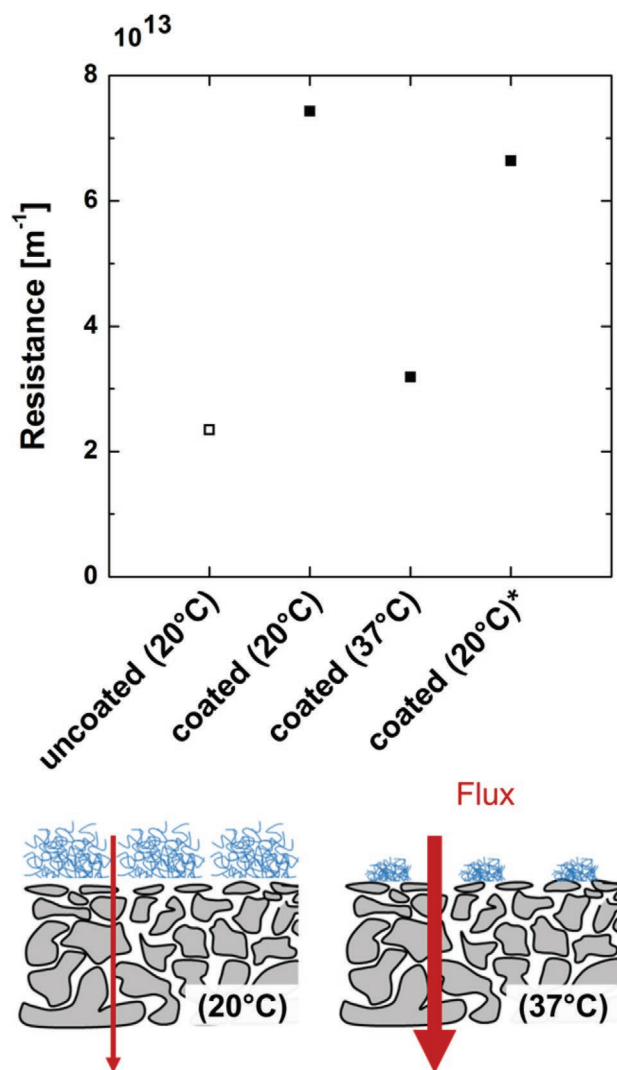


Figure 4. Pure water flux measurements for determining membrane resistance. The thermoresponsiveness of PVCL microgels correlates with the water permeability, as their swelling state tunes membrane resistance. *PVCL coated membranes were steam sterilized at 121 °C for 20 min before pure water flux measurements were conducted.

experiments. **Figure 4** shows pure water resistances through a porous membrane with and without PVCL coating. As expected, the hydraulic resistance increases with the presence of an additional microgel layer on the membrane surface (**Figure 4**). Modulating the swelling state of microgels leads to a tunable permeability. PVCL coated membranes reached resistances of $3.19 \times 10^{-13} m^{-1}$ in the collapsed and $7.43 \times 10^{-13} m^{-1}$ in the swollen state. The uncoated reference membranes showed a resistance of $2.3 \times 10^{-13} m^{-1}$. Even at elevated temperatures of 121 °C, which corresponds to the typical steam sterilization temperature, no detachment of microgels was monitored. The temperature-responsiveness remained unaltered after high-temperature treatment. Moreover, the microgel layer showed to be long term stable when membranes were stored for two weeks. The membrane shows a slight but nonsignificant decline in membrane resistance, which indicates that the

microgels do not desorb from the membrane surface. Here, we could show that a stable and reversible swelling behavior with PVCL microgels can be achieved on PES/PVP membranes by an adsorptive coating process.

2.4. Cell Growth in a Thermoresponsive Hollow Fiber Membrane Bioreactor

Cells were cultured in a custom-made bioreactor and cell growth and tissue formation were investigated on coated and noncoated membranes. Cell morphology clearly shows that cells attach to the PVCL coated membrane and not to the uncoated reference membrane (**Figure 5a,b**). On the reference membrane, cells tend to form globules and agglomerate instead of adhering to the membrane. When culturing cells at 37 °C, the microgels, which are coated on the hydrophilic PES/PVP membranes, are in a collapsed and hydrophobic state. The hydrophobic part of the microgels and the hydrophilic part of the membrane lead to the hypothesis that a patterned surface exists. With this, synergistic effects are utilized like in conventional tissue culture plastic. Polystyrene-based culture surfaces are conventionally used for cell cultivation, but they are originally very hydrophobic, and thus the surface requires post-treated with plasma or corona discharge for better cell adhesion and spreading.^[42] To obtain a more detailed insight about the cell state within the hollow fiber membrane, scanning electron microscopy (SEM) images were taken of sliced hollow fibers (**Figure 5c–e**). In the SEM images, connected cell sheets can be observed. The cells not only grew on the microgel-coated membrane but also appear to produce ECM and form cell connectivity, which resulted in interconnected tissues (**Figure 5c,d**). After cell harvesting, residuals remained on the membrane surface, further supporting the existence of ECM (**Figure 5e**). Within the proposed concept, it is likely that the produced ECM should stay intact after harvesting under physiologic conditions at modest shear stress. Proteolytic enzymes such as trypsin, which are conventionally used in cell cultivation to harvest adherent cells, would lead to cleaved proteins and thus a “cleaned-up” membrane surface. ECM seems not only to be present on the membrane surface, but also within the harvested tissues as they show high reattachment capacity when cultured again on tissue culture plastic (**Figure 7**).

2.5. Harvesting Mini-Tissues in HFMB

Since the PVCL microgels show a beneficial impact on cell attachment (**Figure 5a**), the feasibility to harvest intact 3D cell tissues without using traditional proteolytic enzymes was examined. For harvesting, the HFMB was exposed to room temperature to induce a temperature shift. The module was placed upright and the cold medium was flushed on the shell side of the hollow fibers and stored for one hour. Afterward, shear stress was applied by flushing medium on the lumen side, and the collected tissues were analyzed under a bright field microscope (**Figure 6**). From the images, it can be concluded that interconnected 3D cell tissues were created inside the membrane bioreactor. Tubular like tissues were successfully

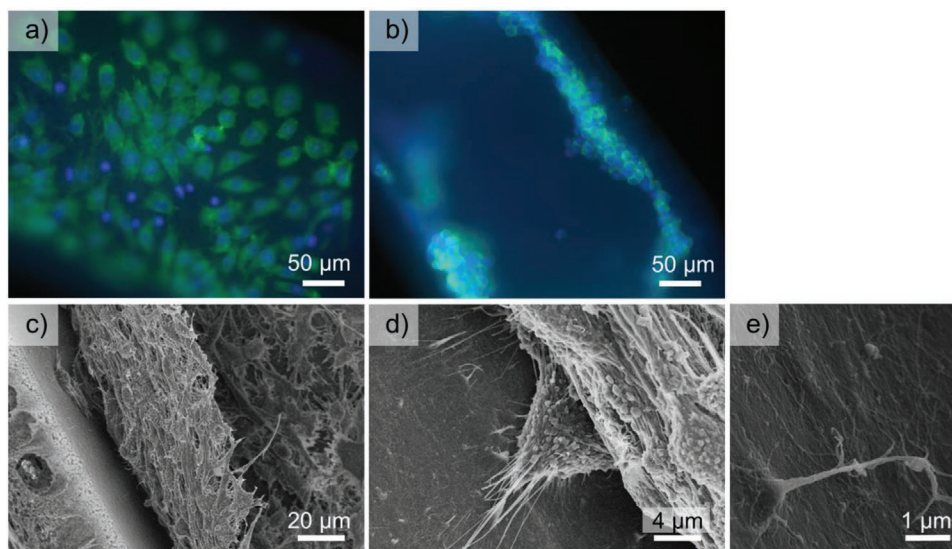


Figure 5. Cell cultivation in an HFMB. a) L929 cell adhesion on PVCL coated and b) noncoated reference membrane. Staining was performed for the nucleolus (blue) and cytoskeleton (green). SEM images of lumen side of the membrane c,d) during cultivation and e) after harvesting.

harvested with lengths >2 mm and had a thickness of ≈ 160 to 180 μm , which is in good agreement with the hollow fiber dimensions (inner diameter 215 μm). More information on tissue thickness determination can be found in the supporting information (Table S2 and Figure S4, Supporting Information). As a comparison, the described harvesting method was also applied for a noncoated membrane. Here, the cells stayed single or formed few cell aggregates (Figure 6c,d) instead of the millimeter-long cell barrels obtained from a microgel-coated membrane. This observation agrees with the cell attachment studies (Figure 5b), where cells poorly attached on a noncoated membrane. It can be concluded that L929 cells express more ECM and build denser intercellular networks when cultivated

on a microgel patched membrane surface with hydrophilic and hydrophobic parts.

From numerous harvesting experiments we could point out two main factors that contribute to the enzyme-free harvesting process in the HFMB system: 1) change in physiochemical property and size of the microgels and 2) shear stress.

When harvesting adherent cells, a force holding the cells on the surfaces needs to be overcome to obtain the cells. Traditionally, this is performed by enzymatic cleavage. However, the enzymatic cleavage not only detaches the cells from a surface but also separates them from the cell network. Here, the adhesive property of temperature-responsive microgels is reduced due to the better solvation of polymer chains with water molecules when falling below the VPTT. This property change is enough to detach whole cell tissues from a thermoresponsive surface. In a first step, proteins from the cell cultivation media adsorb preferentially by the hydrophobic interactions with the alkyl segments of lactam rings in polymer chains localized on the microgel surface to which cells then bind through their integrins. Below the VPTT, the PVCL chains interact more actively with water molecules what leads to the “screening” of the hydrophobic alkyl segments of lactam rings, which causes a desorption effect of the proteins and thus enables cell detachment. It is important to highlight that the electrostatic force resulting from the different potentials between proteins and the polymer substrate plays an essential role in the control of protein adsorption and desorption. This phenomenon is influenced by pH, ionic strength, and temperature, which needs to be considered when using responsive polymers.^[43]

The temperature triggered cell harvesting process can be further enhanced by applying shear stress to the tissues. In a previous work, it was demonstrated that shear stress could promote cell detachment.^[44] Since spontaneous detachment of cell sheets on hydrated polymers takes some time, controlled applied shear stress can accelerate the whole process

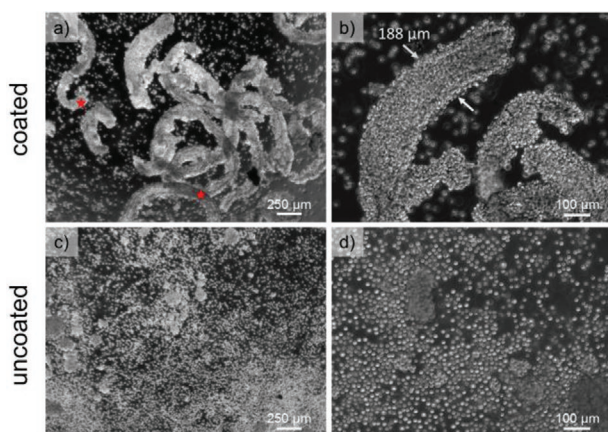


Figure 6. Enzyme-free harvesting of L929 cells cultivated on membranes coated a,b) with and c,d) without PVCL microgels. Red stars represent >1 mm long cell tissues. The length was measured in ImageJ with the setting “segmented line.” Tissue thickness was also analyzed in ImageJ with the setting “straight line.” An overview of the thickness evaluation can be found in Table S2 and Figure S4 in the Supporting Information.

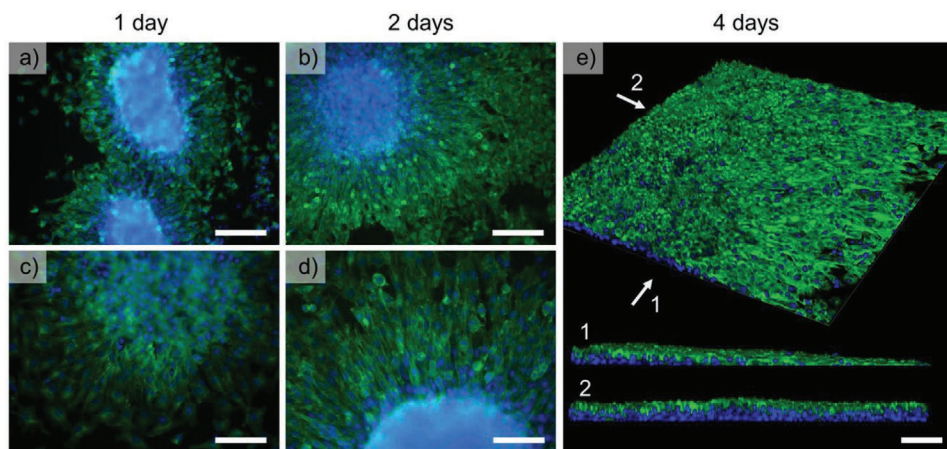


Figure 7. Reseeding of harvested 3D tissues on tissue culture plastic (96 well plate). Fluorescent images were taken with a–d) an apotome and e) confocal microscope. Cell nucleolus (blue), cytoskeleton (green). Scale bar: a,b) 200 μm and c,d,e) 100 μm .

significantly. The groups of Tang et al. and Décavé and Garrivier described that when exceeding a certain threshold stress by applying an external critical force, adhesion bonds can be broken, resulting in cell detachment.^[44–46]

With the HFMB, it is now possible to apply shear stress in a controlled environment by adjusting the flow rate according to the cell type and sensitivity. Hollow fiber membranes, especially in the lumen side, are distinguished by their well-controlled flow profiles at laminar conditions. This well-defined environment allows tissue harvesting at controlled shear stress ranges.

2.6. Reseeding of 3D Tissues from HFMB

After successful enzyme-free harvesting of mini-tissues in the HFMB, the vitality of the obtained cell sheets was proven. The tissues were reseeded on tissue culture plastic to examine the attachment and migration capacity. From the fluorescence images, it can be concluded that healthy tissues were engineered as the cells were able to attach in a successive cultivation (**Figure 7**). Over time, the whole surface area was covered with cells which indicates the migration ability and healthy condition of the tissue. Even after 4 d, cell clusters remained though decreased to three cell layers on top of each other (**Figure 7e**). It seems that the tubular structure of the tissue only remains in the HFMB. Within the HFMB system, the tissue monolayer is stabilized through the membrane support. When tissues are out of the membrane environment, they appear to collapse as the cell monolayer cannot stabilize itself. Also, the collapsing of the tissues goes along with diffusion limitations as the nutrient supply in the center of the tissue is hampered. This observation is supported with the live/dead imaging results where dead cells are solely present in the center part of the harvested tissue (**Figure 8**). In the future, when engineering multilayer tissues, it will be necessary to introduce vasculature within the tissue to overcome diffusion limitations from and to the tissue. Also, it is essential to provide enough surface area for successive cell attachment.

3. Conclusion

The construction of more complex tissues like in cocultivation demand more process intensification than conventional 2D cultivation such as tissue culture plastic can deliver. While tissue culture plastic not only lacks surface area, they are also limited in the nutrient supply with gases and metabolites.

This study successfully demonstrated the feasibility of a temperature-responsive microgel-coated HFMB to harvest large, and interconnected 3D cell tissues without the need of proteolytic enzymes. It was shown that healthy tissues were obtained which attached and proliferated in successive cultivation on standard tissue culture plastic. We identified the driving forces for the harvesting process in the HFMB which is a combination

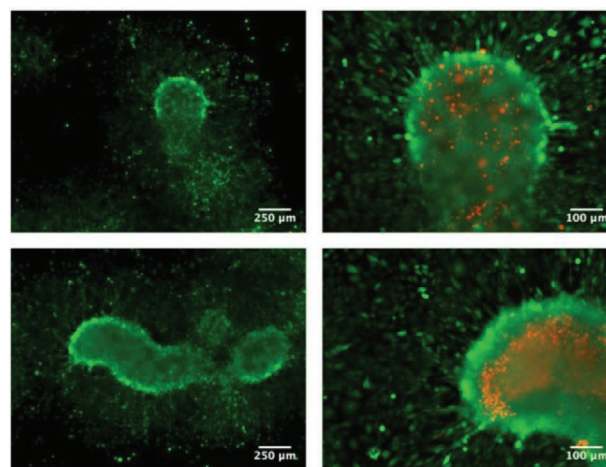


Figure 8. Live/dead images of L929 cells. After harvesting cells were transferred into a 24 well plate and cultured for 2 d with a medium exchange after the first day. From the two image sections (left side) as well as when zooming in (right side), cells not only adhered in successive cultivation but also displayed a high vitality (green cells). As tissues collapse upon detachment, the core of the tissues is subject to diffusion limitation, which leads to cell death (red cells).

of shear stress and change in physiochemical property and size of the microgels.

The HFMB was designed to culture tissues in the lumen side of the membrane due to the prevailing homogenous flow profile and by this performing tissue harvesting under controlled shear stresses. Especially for stem cells this can be important as it is known that shear stress has an impact on cell differentiation.

Furthermore, functionalization or coatings of temperature-responsive microgels can further improve cell tissue fabrication. As an example, a heparin-functionalization can lead to accelerated cell growth due to its affinity to bind several proteins and growth factors.^[47]

4. Experimental Section Experimental details are available in the Supporting Information.

Supporting Information

Supporting Information is available from the Wiley Online Library or from the author.

Acknowledgements

S.D. and T.L. contributed equally to this work. The authors thank K. Faensen for the high-quality SEM images. The critical point drying was kindly performed by Stephan Rütten from the Department of Electron Microscopy, Institute for Pathology at the University Hospital RWTH Aachen University. This article was funded by the Excellence Initiative of the German federal and state governments (Exploratory Research Space Seed Fund OPSF433), Collaborative Research Center Sonderforschungsbereich 985 “Functional Microgels and Microgel Systems” by the German Research Foundation (Deutsche Forschungs-gemeinschaft—DFG).

Open access funding enabled and organized by Projekt DEAL.

Conflict of Interest

The authors declare no conflict of interest.

Keywords

3D tissues, cell adhesion, hollow fiber membrane bioreactors, scaffold-free tissues, temperature-responsive microgels

Received: March 23, 2020

Revised: August 11, 2020

Published online: October 21, 2020

- [1] K. Nishida, M. Yamato, Y. Hayashida, K. Watanabe, K. Yamamoto, E. Adachi, S. Nagai, A. Kikuchi, N. Maeda, H. Watanabe, T. Okano, Y. Tano, *N. Engl. J. Med.* **2004**, *351*, 1187.
- [2] K. Sakaguchi, T. Shimizu, T. Okano, *J. Controlled Release* **2015**, *205*, 83.
- [3] Y. Shiroyanagi, M. Yamato, Y. Yamazaki, H. Toma, T. Okano, *BJU Int.* **2004**, *93*, 1069.
- [4] C. Norotte, F. S. Marga, L. E. Niklason, G. Forgacs, *Biomaterials* **2009**, *30*, 5910.
- [5] L. G. Griffith, M. A. Swartz, *Nat. Rev. Mol. Cell Biol.* **2006**, *7*, 211.
- [6] F. Pampaloni, E. G. Reynaud, E. H. K. Stelzer, *Nat. Rev. Mol. Cell Biol.* **2007**, *8*, 839.

- [7] V. Mironov, R. P. Visconti, V. Kasyanov, G. Forgacs, C. J. Drake, R. R. Markwald, *Biomaterials* **2009**, *30*, 2164.
- [8] T. Takezawa, M. Yamazaki, Y. Mori, T. Yonaha, K. Yoshizato, *J. Cell Sci.* **1992**, *101*, 495.
- [9] N. Yamada, T. Okano, H. Sakai, F. Karikusa, Y. Sawasaki, Y. Sakurai, *Makromol. Chem., Rapid Commun.* **1990**, *11*, 571.
- [10] R. M. Sutherland, *Science* **1988**, *240*, 177.
- [11] R. M. Sutherland, J. A. McCredie, W. R. Inch, *J. Natl. Cancer Inst.* **1971**, *46*, 113.
- [12] F. Hirschhaeuser, H. Menne, C. Dittfeld, J. West, W. Mueller-Klieser, L. A. Kunz-Schughart, *J. Biotechnol.* **2010**, *148*, 3.
- [13] K. Nagase, J. Kobayashi, T. Okano, *J. R. Soc., Interface* **2009**, *6*, S293.
- [14] A. Tamura, J. Kobayashi, M. Yamato, T. Okano, *Biomaterials* **2012**, *33*, 3803.
- [15] M. Karg, T. Hellweg, *Curr. Opin. Colloid Interface Sci.* **2009**, *14*, 438.
- [16] R. Pelton, *J. Colloid Interface Sci.* **2010**, *348*, 673.
- [17] Y. Gao, S. C. F. Au-Yeung, C. Wu, *Macromolecules* **1999**, *32*, 3674.
- [18] M. F. Pittenger, D. E. Discher, B. M. Péault, D. G. Phinney, J. M. Hare, A. I. Caplan, *npj Regen. Med.* **2019**, *4*, 22.
- [19] C. A. V. Rodrigues, T. G. Fernandes, M. M. Diogo, C. L. da Silva, J. M. S. Cabral, *Biotechnol. Adv.* **2011**, *29*, 815.
- [20] A. Kumar, B. Starly, *Biofabrication* **2015**, *7*, 044103.
- [21] R. D. Abbott, D. L. Kaplan, *Trends Biotechnol.* **2015**, *33*, 401.
- [22] N. Liu, R. Zang, S.-T. Yang, Y. Li, *Eng. Life Sci.* **2014**, *14*, 4.
- [23] T. L. Place, F. E. Domann, A. J. Case, *Free Radical Biol. Med.* **2017**, *113*, 311.
- [24] N. V. Chevtchik, M. Fedecostante, J. Jansen, M. Mihajlovic, M. Wilmer, M. Rütth, R. Masereeuw, D. Stamatialis, *Eur. J. Pharmacol.* **2016**, *790*, 28.
- [25] D. Janke, J. Jankowski, M. Rütth, I. Buschmann, H. D. Lemke, D. Jacobi, P. Knaus, E. Spindler, W. Zidek, K. Lehmann, V. Jankowski, *PLoS One* **2013**, *8*, e57227.
- [26] D. F. Stamatialis, B. J. Papenburg, M. Gironés, S. Saiful, S. N. M. Bettahalli, S. Schmitmeier, M. Wessling, *J. Membr. Sci.* **2008**, *308*, 1.
- [27] N. M. S. Bettahalli, H. Steg, M. Wessling, D. Stamatialis, *J. Membr. Sci.* **2011**, *371*, 117.
- [28] N. M. S. Bettahalli, N. Groen, H. Steg, H. Unadkat, J. d. Boer, C. A. v. Blitterswijk, M. Wessling, D. Stamatialis, *J. Tissue Eng. Regen. Med.* **2014**, *8*, 106.
- [29] N. M. S. Bettahalli, J. Vicente, L. Moroni, G. A. Higuera, C. A. Van Blitterswijk, M. Wessling, D. F. Stamatialis, *Acta Biomater.* **2011**, *7*, 3312.
- [30] H. Eghbali, M. M. Nava, D. Mohebbi-Kalhari, M. T. Raimondi, *Int. J. Artif. Organs* **2016**, *39*, 1.
- [31] R. Pelton, *Adv. Colloid Interface Sci.* **2000**, *85*, 1.
- [32] D. I. Phua, K. Herman, A. Balaceanu, J. Zakrevski, A. Pich, *Langmuir* **2016**, *32*, 3867.
- [33] a) M. Kather, M. Skischus, P. Kandt, A. Pich, G. Conrads, S. Neuss, *Angew. Chem., Int. Ed.* **2017**, *56*, 2497; b) M. Kather, M. Skischus, P. Kandt, A. Pich, G. Conrads, S. Neuss, *Angew. Chem.* **2017**, *129*, 2537.
- [34] J. B. Thorne, G. J. Vine, M. J. Snowden, *Colloid Polym. Sci.* **2011**, *289*, 625.
- [35] M. Stieger, W. Richtering, J. S. Pedersen, P. Lindner, *J. Chem. Phys.* **2004**, *120*, 6197.
- [36] M. Zhuang, T. Liu, K. Song, D. Ge, X. Li, *Mater. Sci. Eng., C* **2015**, *55*, 410.
- [37] J. Ramos, A. Imaz, J. Forcada, *Polym. Chem.* **2012**, *3*, 852.
- [38] H. Vihola, A. Laukkanen, L. Valtola, H. Tenhu, J. Hirvonen, *Biomaterials* **2005**, *26*, 3055.
- [39] a) D. Menne, F. Pitsch, J. E. Wong, A. Pich, M. Wessling, *Angew. Chem., Int. Ed.* **2014**, *53*, 5706; b) D. Menne, F. Pitsch, J. E. Wong, A. Pich, M. Wessling, *Angew. Chem.* **2014**, *126*, 5814.

- [40] M. Barth, M. Wiese, W. Ogieglo, D. Go, A. J. C. Kuehne, M. Wessling, *J. Membr. Sci.* **2018**, 555, 473.
- [41] T. Lohaus, P. de Wit, M. Kather, D. Menne, N. E. Benes, A. Pich, M. Wessling, *J. Membr. Sci.* **2017**, 539, 451.
- [42] A. S. Curtis, J. V. Forrester, C. McInnes, F. Lawrie, *J. Cell Biol.* **1983**, 97, 1500.
- [43] H. Kawaguchi, K. Kisara, T. Takahashi, K. Achiha, M. Yasui, K. Fujimoto, *Macromol. Symp.* **2000**, 151, 591.
- [44] Z. Tang, Y. Akiyama, K. Itoga, J. Kobayashi, M. Yamato, T. Okano, *Biomaterials* **2012**, 33, 7405.
- [45] E. Décavé, D. Garrivier, Y. Bréchet, B. Fourcade, F. Bruckert, *Biophys. J.* **2002**, 82, 2383.
- [46] D. Garrivier, E. Décavé, Y. Bréchet, F. Bruckert, B. Fourcade, *Eur. Phys. J. E* **2002**, 8, 79.
- [47] Y. Arisaka, J. Kobayashi, M. Yamato, Y. Akiyama, T. Okano, *Biomaterials* **2013**, 34, 4214.